Stronger role of four-phonon scattering than three-phonon scattering in thermal conductivity of III-V semiconductors at room temperature

Xiaolong Yang,[1,2,3] Tianli Feng,[1,4] Ju Li,[5] and Xiulin Ruan[1,*]

[1]*School of Mechanical Engineering and the Birck Nanotechnology Center, Purdue University, West Lafayette, Indiana 47907-2088, USA*

[2]*Institute for Advanced Study, Shenzhen University, Nanhai Avenue 3688, Shenzhen 518060, China*

[3]*Frontier Institute of Science and Technology, and State Key Laboratory for Mechanical Behavior of Materials, Xi'an Jiaotong University, Xi'an 710049, China*

[4]*Center for Nanophase Materials Sciences, Oak Ridge National Laboratory, Oak Ridge, Tennessee 37831, USA*

[5]*Department of Nuclear Science and Engineering and Department of Materials Science and Engineering, Massachusetts Institute of Technology, Cambridge, Massachusetts 02139, USA*

(Received 15 August 2019; revised manuscript received 22 October 2019; published 9 December 2019)

Recent studies reveal that four-phonon scattering can be important in determining thermal conductivities of solids. However, these studies have been focused on materials where the thermal conductivity κ is dominated by acoustic phonons, and the role of four-phonon scattering, although significant, is still smaller than that of three-phonon scattering at room temperature. In this work, taking AlSb as an example for which optical phonons contribute significantly to the thermal conductivity under the three-phonon picture, we demonstrate that four-phonon scattering can be more important than three-phonon scattering as it diminishes optical phonon thermal transport and therefore significantly reduces the thermal conductivities of materials. Also, our calculations show that four-phonon scattering can diminish the isotope effect on κ. Specifically, including four-phonon scattering reduces the room-temperature κ of isotopically pure BAs from 3322 W/mK to 1721 W/mK, a 48% reduction. Four-phonon scattering reduces the room-temperature κ of the isotopically pure and naturally occurring AlSb by 70% and 50%, respectively, indicating that four-phonon scattering is more important than three-phonon scattering. The reductions for isotopically pure and naturally occurring cubic GaN are about 34% and 27%, respectively. For isotopically pure wurtzite GaN, the reduction is about 13% at room temperature and 25% at 400 K. These results provided important guidance for experimentalists for achieving high thermal conductivities in III-V compounds for applications in the semiconductor industry.

DOI: 10.1103/PhysRevB.100.245203

I. INTRODUCTION

III-V compound semiconductors including AlSb, BAs, and GaN, have attracted remarkable attention due to their extraordinary electronic, thermal, and optical behaviors, with great potential for applications in high-power electronics [1], optoelectronic devices [2], and thermal management [3,4]. In particular, owing to the peculiar phonon band structure such as a large acoustic-optical (a-o) band gap, acoustic bunching, and the flatness of the optical branches, these materials tend to exhibit unusually high thermal conductivity, which thus makes them promising candidates for heat dissipation in nanoelectronics as microelectronic devices shrink [5]. To this end, in recent years thermal transport in III-V compounds has been extensively investigated both in experiments and in theory. Recently, first-principles calculations based on the solution of the phonon Boltzmann transport equation (BTE) have made significant progress in terms of accurately predicting the lattice thermal conductivity of a great number of semiconductor systems [6–12]. For instance, by combining the density functional calculations and the linearized BTE, Lindsay and co-workers have calculated lattice thermal conductivities of cubic aluminum-V, gallium-V, and indium-V compounds based on the lowest anharmonic phonon scattering [13]. They performed anharmonic lattice dynamics calculations based on density functional theory (DFT) to predict thermal conductivities of wurtzite GaN and cubic GaN [14]. With the same approach, they also examined the thermal conductivities and isotope effects of cubic III-V boron compounds [15]. Despite great efforts to study thermal transport in III-V compounds, however, due to ignoring higher-order four-phonon scattering, these previous works usually give considerable overestimation of thermal conductivities as compared to experimental measurements at higher temperatures or even room temperature (RT). For instance, the zinc-blende BAs was predicted to have a thermal conductivity of ∼2200 W/mK at RT with three-phonon scattering, much higher than the experimental value [15]. Also, the previous prediction on thermal conductivity of cubic AlSb within three-phonon theory is as high as 100 W/mK at RT [13], which is substantially higher than the value measured by experiment, ∼50 W/mK [16].

Only recently a formalism to explicitly determine four-phonon scattering from perturbation theory was developed [17], and it was demonstrated that four-phonon processes can actually remedy the discrepancies between the previous calculation and experiments and even play a dominant role at high temperature [18,19]. Notably, the predicted BAs thermal conductivity κ has recently been confirmed by experiments [20–22], stimulating the wide acceptance of the

*ruan@purdue.edu

four-phonon scattering theory. Recent works of combining both four-phonon scattering and phonon renormalization have also appeared [23,24]. Although the research techniques of predicting thermal conductivity of semiconductor materials are gradually maturing, nonetheless, thermal transport properties of III-V compounds such as AlSb, cubic GaN (c-GaN), and wurtzite GaN (w-GaN) are still not well understood. In this context, it is of fundamental importance to revisit their lattice thermal conductivities by considering previously neglected four-phonon scattering. Moreover, we note that a few recent studies [18,19,25] within the framework of four-phonon theory have been mainly focused on materials where κ is dominated by acoustic phonons, e.g., BAs [18], and the impact of four-phonon scattering, although significant, is still generally smaller than that of three-phonon scattering.

Of particular note is that some previous predictions indicate that the optical phonons provide major contributions to κ in some III-V semiconductors such as the aluminum-V compounds [10,12,26]. A typical example is zinc-blende AlSb: Lindsay *et al*. have demonstrated that optical phonons contribute more than the acoustic phonons to the total κ even at RT [13]. This is in sharp contrast to BAs for which acoustic phonons dominate thermal conductivity. However, their prediction was limited to only three-phonon scattering. Hence, it is worth exploring two open questions in such optical phonon-dominated thermal materials.

(1) How much does the four-phonon scattering impact the overall thermal conductivity?

(2) How much does the four-phonon scattering impact the relative contributions of optical phonons?

Additionally, as aforementioned above, semiconductors like BAs, AlSb, c-GaN, and w-GaN have unique phonon band features (i.e., the large a-o gap, acoustic bunching, and the flatness of the optical bands, etc.), which make the satisfaction of three-phonon selection rules quite difficult if not impossible. This will weaken the coupling or interaction between acoustic and optical phonons and lead to relatively strong phonon-isotope scattering, rendering the large isotope effect on κ in these materials [13–15,26]. For instance, Lindsay *et al*. have predicted with only lowest-order anharmonicity that the isotope effect in w-GaN is very large, and at around 30 K the calculated κ for isotopically pure GaN is almost 7 times higher than that with naturally occurring isotope concentration [26]. In essence, the origin of the isotope effect is the interplay between the intrinsic anharmonic phonon-phonon scattering and phonon-isotope scattering. Although the three-phonon process is largely restricted by the peculiar phonon structure, higher-order four-phonon scattering, however, cannot be restricted by these band characteristics [18]. Thus, a natural question is as follows: how does four-phonon scattering change the role of the isotope effect in these materials?

In this work, by solving the linearized phonon BTE based on first-principles calculations, we systematically study the lattice thermal conductivities and isotope effects in BAs, AlSb, c-GaN, and w-GaN with four-phonon scattering included. Particularly, we demonstrate that after considering four-phonon scattering in AlSb, the relative contribution of optical phonons to thermal conductivity diminishes. This leads to about 50% reduction in κ of naturally occurring AlSb even at RT, indicating that unlike in BAs, four-phonon scattering plays a dominant role over three-phonon scattering in AlSb. Further phonon scattering analysis shows that four-phonon processes can play a dominant role in the intrinsic resistance for optic phonons, due to the highly restrictive selection rules of three-phonon scattering. The interplay of intrinsic phonon-phonon scattering and phonon-isotope scattering is also discussed by highlighting the role of four-phonon scattering in determining the κ of these four materials. Also, by comparison with AlSb, BAs, c-GaN, and w-GaN, we demonstrate that the interplay among the large a-o gap, bunching of acoustic branches, and low-frequency optical bands together decides the importance of four-phonon scattering in thermal transport.

II. COMPUTATIONAL DETAILS

Within the framework of the BTE [27], the lattice thermal conductivity κ along the transport direction can be determined by summing up the contributions from each phonon branch α and integrating over the first Brillouin zone (BZ) [26,28],

$$\kappa = \frac{1}{k_B T^2}\frac{1}{8\pi^3}\sum_{\alpha}\int_{BZ} f_0(\omega_{\alpha,\mathbf{q}})[f_0(\omega_{\alpha,\mathbf{q}})+1] \times \upsilon^2_{\alpha,\mathbf{q}}\hbar^2\omega^2_{\alpha,\mathbf{q}}\tau_{\alpha,\mathbf{q}}d\mathbf{q}, \quad (1)$$

where $\upsilon_{\alpha,\mathbf{q}}$ is the phonon group velocity along the transport direction, $\tau_{\alpha,\mathbf{q}}$ is the phonon lifetime, and f_0 denotes the phonon occupation number that obeys the Bose-Einstein distribution.

To obtain accurate κ, we employ an iterative scheme mixing three-phonon scattering to exactly solve the phonon BTE based on *ab initio* calculations [6,15,29], by considering isotopic scattering and intrinsic anharmonicity up to fourth order. To effectively reduce the computational cost, herein four-phonon scattering rates τ_4^{-1} are included into the iterative scheme within the relaxation time approximation level, which has been demonstrated to be valid when four-phonon scattering is dominated by Umklapp processes [18].

Solving the numerical phonon BTE requires accurate calculations of the harmonic and anharmonic interatomic force constants (IFCs), which are obtained from DFT within the local density approximation using the first-principle-based VASP package [30–32]. The harmonic IFCs are calculated using $4\times4\times4$ supercells and a $4\times4\times4$ Monkhorst-Pack grid within a finite displacement scheme, as implemented in the open source software package PHONOPY [33]. The nonanalytical term is included to capture longitudinal optical (LO) /transverse optical (TO) splitting for all the materials studied. The third-order IFCs are calculated through THIRDORDER [28], a package of Sheng BTE, considering up to the fifth-nearest neighbor. The fourth-order IFCs are calculated out to the second-nearest neighbors. The $4\times4\times4$ primitive cells and the $4\times4\times4$ Monkhorst-Pack grid are adopted to calculate the third and fourth IFCs from a finite differences method. With these IFCs, the phonon frequencies and velocities are then obtained by diagonalizing the dynamical matrix, and the phonon scattering rates are calculated from the iterative solution of the BTE described above. The thermal conductivity is solved with a $16\times16\times16$ $\mathbf{q}$-mesh. In the cell relaxation, the total energy and Hellmann-Feynman force convergence thresholds are set to 10^{-10} eV and 10^{-6} eV/Å,

TABLE I. Experimental and calculated lattice constants for AlSb, BAs, c-GaN, and w-GaN.

Lattice constant (Å)	AlSb	BAs	c-GaN	w-GaN
a_{calc} (a_{exp})	6.12 (6.14 [34])	4.81 (4.78 [20])	4.55 (4.50 [14])	3.16 (3.19 [35])
c_{calc} (c_{exp})				5.15 (5.19 [35])

respectively. The optimized lattice constants a and c for each material examined here are in good agreement with experiments [14,22,34,35], as listed in Table I. The energy cutoff is determined by adding 30% to the highest energy cutoff for the pseudopotentials. The expressions for all involved scattering rates in this work have been given in detail previously [18,19].

III. RESULTS AND DISCUSSION

A. Phonon dispersions

The calculated phonon dispersions of AlSb, BAs, c-GaN, and w-GaN along the high-symmetry directions are plotted in Fig. 1. For AlSb, BAs, and c-GaN, the phonon dispersions are very similar along the main high-symmetry **q** points in the irreducible BZ. There exist 3 acoustic and 3 optical phonon branches corresponding to the two atoms per primitive cell, separated into two parts by the large phonon band gap due to the mass difference between the component elements. For w-GaN, the 12 phonon branches corresponding to the four atoms in the primitive cell are also separated into two parts by a large band gap, of which the upper parts are 6 optical branches while the lower ones include 3 acoustic branches and 3 optical branches. In these materials, the large band gap will forbid two acoustic phonons combining into an optical phonon and thus weaken the coupling between acoustic and optical phonons, due to the strong restriction of simultaneous energy and momentum conservations. However, it will not be restrictive for four-phonon processes between acoustic and optical phonons. As illustrated in the case of BAs in Fig. 1, the recombination processes of four-phonon scattering can easily occur.

In addition to the large band gap, we also see that in BAs the three acoustic branches in the frequency range from 4 to 10 THz are close to each other like a bunching, which will suppress the phase space for the three-acoustic-phonon scattering channels (so-called *aaa* scattering) since the summation of the energies of two acoustic phonons can hardly reach that of the acoustic phonon, as proven previously [15,18]. Unlike BAs, the three acoustic branches in AlSb are relatively dispersive, implying the stronger *aaa* scattering phase space in AlSb. Besides, the phonon dispersions of these four materials exhibit the salient flatness of the optical branches, especially for AlSb, which will largely weaken three-optical-phonon scattering processes (so called *ooo* scattering) due to the energy selective rule. Also, the flatness of the optical band reflects that these materials have relatively small group velocities of optical modes. Conventionally, optical phonons should have little

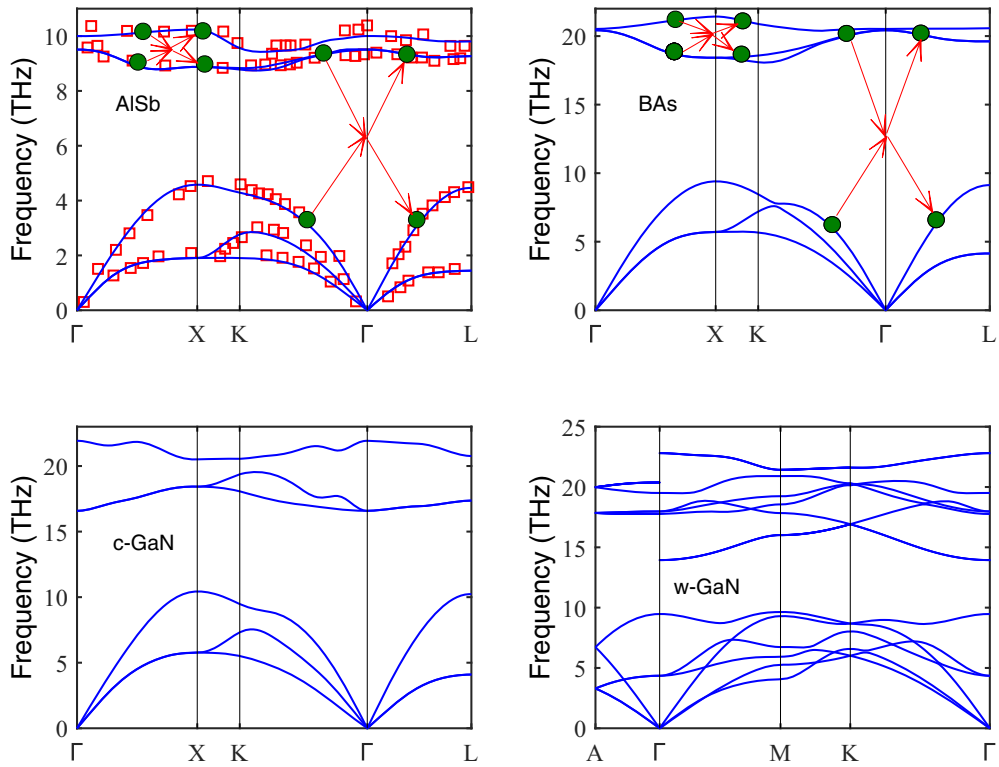

FIG. 1. Phonon dispersions of AlSb, BAs, c-GaN, and w-GaN along high-symmetry directions in the BZ. The solid lines are the results from *ab initio* calculations in this work. The red squares are experimental data points for AlSb from Ref. [36]. Green circles and red arrows illustrate the recombination channels of four-phonon scattering processes in AlSb and BAs.

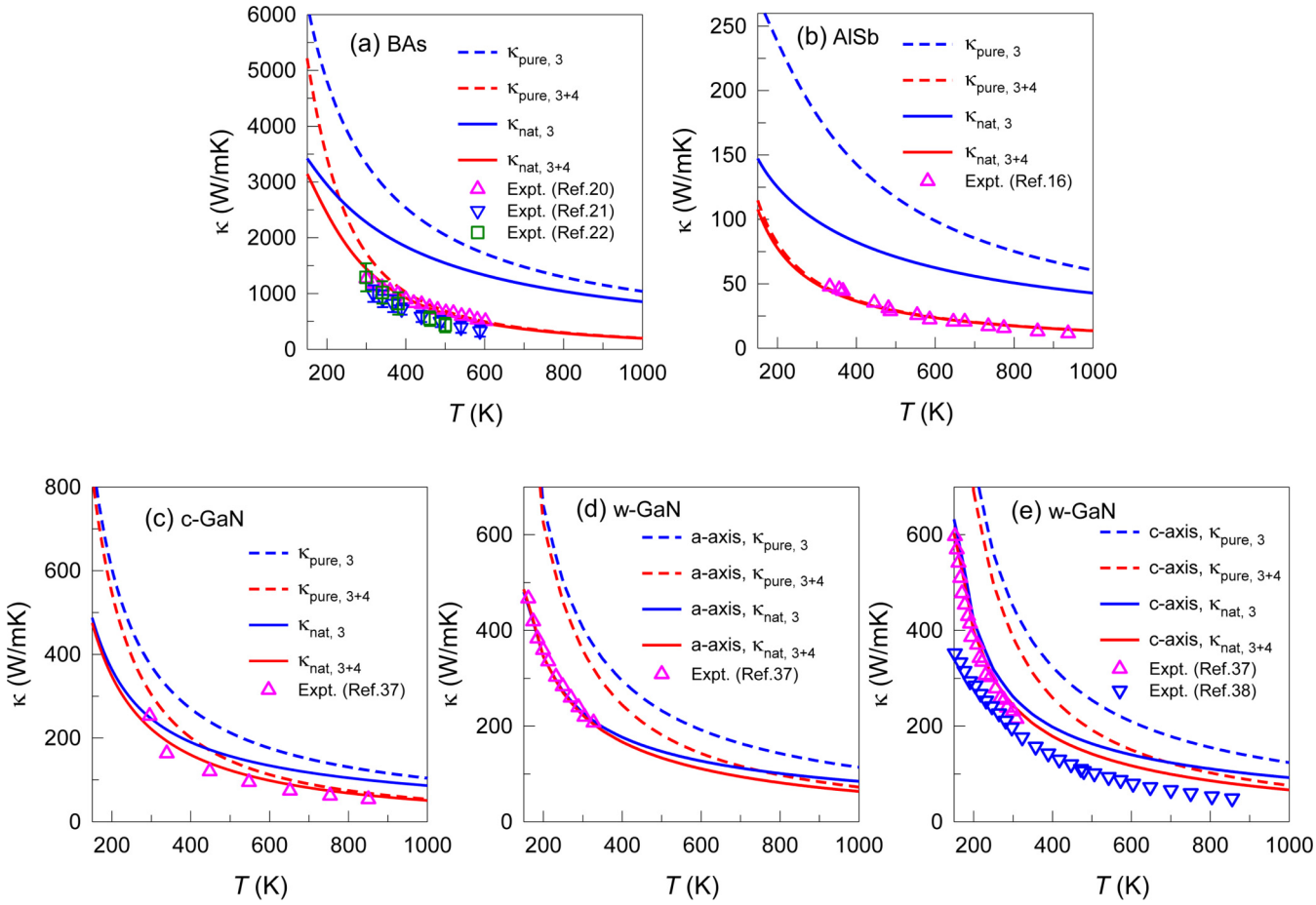

FIG. 2. Lattice thermal conductivity as a function of temperature for BAs (a), AlSb (b), cubic GaN (c), and wurtzite GaN along different directions (d, e). The Dashed lines represent the calculated κ for isotopically pure materials (κ_{pure}) and the solid lines represent the calculated κ with naturally occurring materials (κ_{nat}). The blue lines give the calculated κ with only three-phonon scattering and the red lines give the results after including four-phonon scattering. All symbols represent experimental data for naturally occurring materials from Refs. [16,20–22,37,38].

contribution to their lattice thermal conductivities. However, what makes AlSb stand out is that based on previous work [13] optical phonons make a dominant contribution to κ over acoustic phonons even at RT. Consequently, we concluded that the large contribution of optical modes to κ in AlSb probably originates not from large velocities, but from the large lifetimes of optical modes, since in AlSb *aao*- and *ooo*-scattering channels are suppressed by the large a-o gap and the flatness of the optical bands, and *aoo* scattering actually provides the only intrinsic resistance for optical phonons. Hence, four-phonon scattering may become non-negligible for the optical contributions to κ.

B. Comparison with experimental results

Our main results are shown in Fig. 2. The calculated κ values with four-phonon scattering included are compared with those without the four-phonon term for naturally occurring BAs, AlSb c-GaN, and w-GaN, as well as with corresponding isotopically pure materials. Blue curves are calculated results with anharmonicity up to third order for isotopically pure materials $\kappa_{\text{pure},3}$ (dashed lines) and for naturally occurring materials $\kappa_{\text{nat},3}$ (solid lines). Red curves give the calculated results after including four-phonon scattering for isotopically pure materials $\kappa_{\text{pure},3+4}$ (dashed lines) and for naturally occurring materials $\kappa_{\text{nat},3+4}$ (solid lines). All symbols represent the measured κ of Refs. [16,20–22,37,38]. Also, for ease of appreciating the significance of four-phonon scattering, our calculated RT values of κ_{pure} and κ_{nat} for these four materials are shown in Table II.

In terms of naturally occurring materials, it is found that for both BAs and AlSb, when anharmonicity is considered

TABLE II. The calculated RT $\kappa_{\text{nat},3}$, $\kappa_{\text{nat},3+4}$, $\kappa_{\text{pure},3}$, and $\kappa_{\text{pure},3+4}$, and the percent isotope effect P for AlSb, BAs, c-GaN, and w-GaN.

Material	κ_{pure} (W/mK)		κ_{natural} (W/mK)		P(%)	
	$\kappa_{\text{pure},3}$	$\kappa_{\text{pure},3+4}$	$\kappa_{\text{nat},3}$	$\kappa_{\text{nat},3+4}$	P_3	P_4
AlSb	181	51	99	50	83.3	3.2
BAs	3322	1721	2276	1441	46.0	19.4
c-GaN	372	304	246	222	51.2	37.2
w-GaN, *a* axis	406	359	228	223	78.2	61.1
w-GaN, *c* axis	450	385	261	243	72.2	58.6

up to third order, the values of thermal conductivity $\kappa_{\text{nat},3}$ are much overestimated over the entire temperature range as compared to the experimental data [16,22]. With four-phonon scattering included, our prediction yields the $\kappa_{\text{nat},3+4}$ values in reasonable agreement with experimental measurements. This indicates that four-phonon processes can be responsible for the discrepancies between previous calculations and experiments. For BAs when four-phonon scattering is included, the calculated RT $\kappa_{\text{nat},3+4}$ will decrease by ∼37%, and the magnitude is reduced from 2276 to 1441 W/mK, which is quantitatively consistent with previous work [18,22]. Particularly, in AlSb we find that four-phonon scattering dramatically lowers the value of RT κ_{nat} from 99 to 50 W/mK, by almost 50%, demonstrating the stronger role of four-phonon scattering in AlSb than in BAs.

As is seen from Figs. 2(c)–2(e), for c-GaN and w-GaN, although four-phonon scattering is not as important as that in BAs and AlSb, it still plays a non-negligible role in determining κ, especially at high temperatures. For natural occurring c-GaN and w-GaN, three-phonon predictions can yield the values of κ in good accordance with experiments below RT. As T rises, however, obvious deviations from experiment occur. At RT, in c-GaN three-phonon predicted values ($\kappa_{\text{nat},3} = 246$ W/mK and $\kappa_{\text{pure},3} = 372$ W/mK) are higher than those of four-phonon theory ($\kappa_{\text{nat},3+4} = 222$ W/mK and $\kappa_{\text{pure},3} = 304$ W/mK). Similarly, in w-GaN the three-phonon theory gives RT values ($\kappa_{\text{nat},3} = 228$ W/mK and $\kappa_{\text{pure},3} = 406$ W/mK along the a axis, $\kappa_{\text{nat},3} = 261$ W/mK and $\kappa_{\text{pure},3} = 450$ W/mK along the c axis), whereas four-phonon theory presents the lower results with $\kappa_{\text{nat},3+4} = 223$ W/mK and $\kappa_{\text{pure},3+4} = 359$ W/mK along the a axis, and $\kappa_{\text{nat},3+4} = 243$ W/mK and $\kappa_{\text{pure},3+4} = 385$ W/mK along the c axis, respectively. At temperatures above 400 K, our prediction of κ including four-phonon scattering deviates significantly from that only involving three-phonon scattering. For c-GaN in particular, at around 850 K, the three-phonon prediction alone gives $\kappa \sim 99$ W/mK, much larger than the experimental value, 54 W/mK [37]. After including four-phonon scattering, our prediction can agree well with available measurement [37] in the whole T range. The disagreement between experiment [38] and our theoretical calculation for w-GaN in Fig. 2(e) may be attributed to some defects in experimental samples such as dislocations and impurities. We note that temperature-induced phonon renormalization has recently been found to be important in materials with strong anharmonicity, such as PbTe [23] and NaCl [24]. However, we expect this effect to have little impact on our results, since the systems studied here are strongly harmonic materials.

Another point worth noting in Fig. 2 is that the phonon-isotope scattering has a large impact on thermal conductivities for these four materials studied. Comparing κ_{nat} and κ_{pure} of these materials, we can see that with only three-phonon scattering considered, phonon-isotope scattering can greatly reduce thermal conductivities, especially for low temperatures. As seen in Table II, AlSb has $\kappa_{\text{pure},3} = 181$ W/mK around RT, being almost 2 times higher than $\kappa_{\text{nat},3} = 99$ W/mK. For BAs, $\kappa_{\text{pure},3}$ at RT is 3322 W/mK, far larger than $\kappa_{\text{nat},3} = 2276$ W/mK. In c-GaN, $\kappa_{\text{pure},3}$ at RT is 372 W/mK, much higher than $\kappa_{\text{nat},3} = 246$ W/mK. For w-GaN, the RT $\kappa_{\text{pure},3}$ along the a axis and c axis are 406 and 450 W/mK, respectively, being almost 2 times larger than the corresponding $\kappa_{\text{nat},3}$. This intriguing finding is due to the interplay between the phonon-phonon and phonon-isotope scattering. In these materials the anharmonic three-phonon scattering is relatively weak and the phonon-isotope scattering is relatively more important, due to the large a-o gap and atomic mass difference. Obviously, we find that after considering four-phonon scattering the isotope effects become less important, but certainly still cannot be neglected. Inclusion of four-phonon scattering makes the intrinsic anharmonic phonon scattering stronger, thus weakening the relative contribution of phonon-isotope scattering to κ. We can clearly see from Table II that at RT $\kappa_{\text{pure},3+4} = 51$ W/mK and $\kappa_{\text{nat},3+4} = 50$ W/mK for AlSb, and $\kappa_{\text{pure},3+4} = 1721$ W/mK and $\kappa_{\text{nat},3+4} = 1441$ W/mK for BAs. For both c-GaN and w-GaN, it is quite different from AlSb and BAs that even after including four-phonon scattering the values of $\kappa_{\text{pure},3+4}$ are still much larger than those of $\kappa_{\text{nat},3+4}$, as listed in Table II, indicating the strong isotope effect in these two systems.

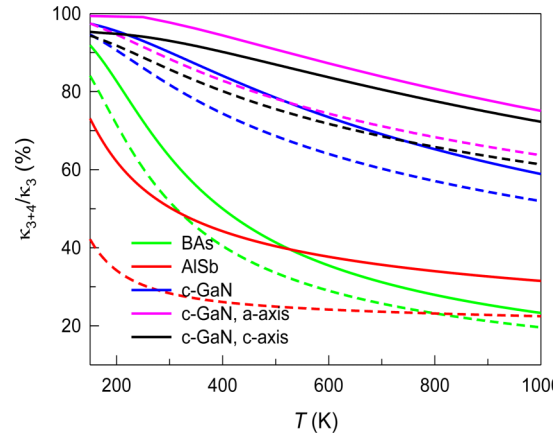

FIG. 3. The relative thermal conductivities κ_{3+4}/κ_3 as a function of T for BAs, AlSb, c-GaN, and w-GaN. Solid curves correspond to calculated κ_{nat} and dashed curves correspond to κ_{pure}.

To see it more clearly, Fig. 3 shows the relative thermal conductivity κ_{3+4}/κ_3 with respect to T. The solid curves correspond to the results for materials with naturally occurring isotopic abundances, and the dashed curves are for isotopically pure materials. By contrast, it can be concluded that four-phonon scattering is more significant in lowering thermal conductivity for isotopically pure materials than for naturally occurring materials. For AlSb in particular, the RT thermal conductivity of isotopically pure material decreases by more than 70%, larger than the 50% reduction in the naturally occurring case.

C. Four-phonon scattering diminishes the optical phonon contribution in AlSb

To gain further insight into the giant κ reduction in AlSb induced by four-phonon scattering, we display the contribution of different phonon branches to κ_{nat} with respect to T, as shown in Fig. 4 and Table III. We clearly see from Fig. 4(a) that with only three-phonon scattering included, in AlSb the optical branches dominate κ over the acoustic branches even at 250 K, and more so at higher temperatures. Surprisingly,

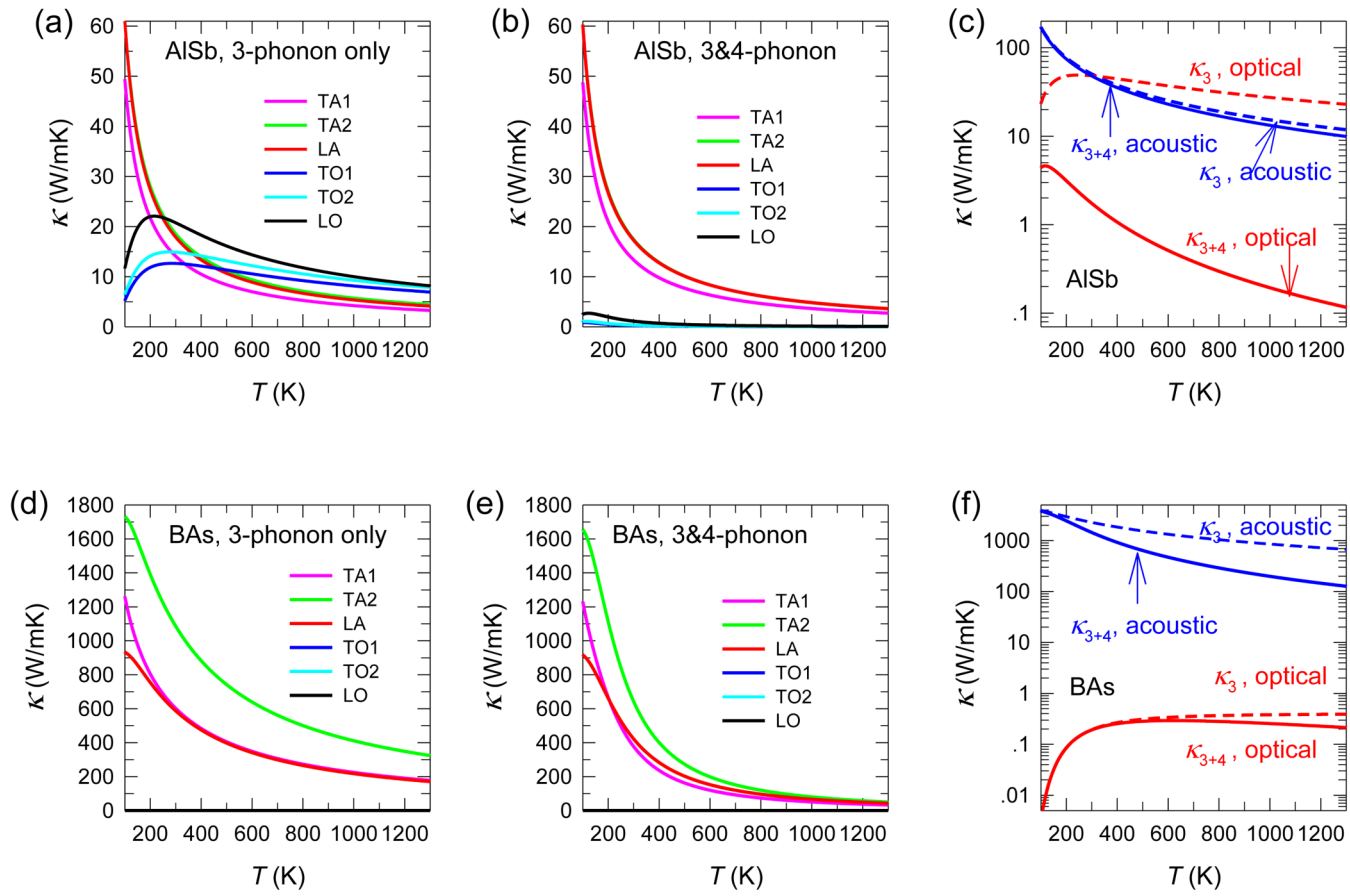

FIG. 4. T-dependent κ_{nat} of each branch for AlSb and BAs with τ_4^{-1} (b, e) and without τ_4^{-1} (a, d). The contribution to κ_{nat} from total acoustic branches and total optical branches for AlSb (c) and BAs (f).

as is seen in Fig. 4(b), after including four-phonon scattering, not only does the acoustic phonon contribution decreases to some extent but also, more importantly, the contribution of all optical modes to κ almost vanishes. This is because of the large four-phonon scattering phase space of optical phonons in AlSb due to the flatness of the optical branches, which is discussed in more detail later.

For a clearer insight we plot the contributions to κ from total acoustic modes (blue lines) and total optical modes (red lines) with respect to T in Fig. 4(c). We see that in AlSb four-phonon scattering has a much larger impact on optical phonons than on acoustic phonons in reducing κ, while BAs exhibits the opposite pattern [see Fig. 4(f)]. Specifically, after including four-phonon scattering, in AlSb the acoustic contribution to κ at RT makes little change, whereas the counterpart of the optical contribution is almost fully eliminated. In contrast, in BAs four-phonon scattering leads to an ∼37% reduction in acoustic contribution and it can be neglected for optical modes which have negligible contribution to κ.

In Table III, we note that in AlSb the relative contribution of all optical branches at 300 K decreases from 48.9% to 3.6% after including four-phonon scattering. The contribution of all acoustic branches increases from 51.1% to 96.4%. Even when

TABLE III. Percentage contribution of different phonon branches to κ for naturally occurring AlSb and BAs at 300 and 1000 K, respectively.

		300 K		1000 K	
Material	κ%	Three-phonon only	Three- and four-phonon	Three-phonon only	Three- and four-phonon
AlSb	TA1	14.26%	26.91%	9.89%	27.05%
	TA2	18.77%	34.65%	13.42%	34.09%
	LA	18.09%	34.83%	12.52%	36.78%
	Optical	48.88%	3.61%	64.17%	2.08%
BAs	TA1	28.35%	27.46%	28.27%	26.52%
	TA2	47.64%	44.77%	47.94%	40.86%
	LA	24%	27.75%	23.73%	32.45%
	Optical	0.01%	0.02%	0.06%	1.7%

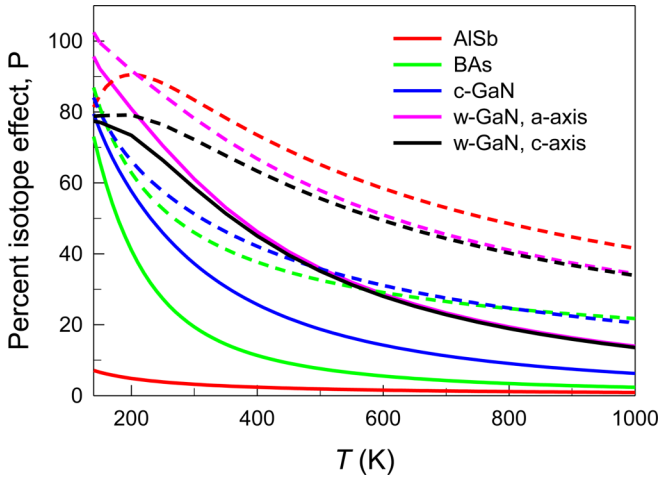

FIG. 5. Calculated isotope effect, $P = (\kappa_{\text{pure}}/\kappa_{\text{nat}} - 1) \times 100\%$, versus temperature for AlSb (red line), BAs (blue line), c-GaN (pink line), and w-GaN (green line). Dashed lines give the results with only three-phonon scattering, and solid lines give the results after including four-phonon scattering.

T increases to 1000 K, the relative contribution of optical modes accounts for only ∼2%. This suggests that the previous prediction based on three-phonon theory, showing that optical phonons contributed considerably to the κ of AlSb, is actually misleading. Four-phonon scattering theory indicates that the κ of AlSb is still primarily governed by acoustic phonons, and optical phonons have little direct contribution to κ. In the case of BAs, unlike AlSb, one can see from Figs. 4(d)–4(f) that, whether or not the four-phonon scattering is included, the acoustic phonons always dominate the thermal conductivity κ.

D. Four-phonon scattering weakens the isotope effect

We then show the calculated isotope effect, defined by $P = (\kappa_{\text{pure}}/\kappa_{\text{nat}} - 1) \times 100\%$, versus T for AlSb (red lines), BAs (green lines), c-GaN (blue lines), and w-GaN (pink and black lines) in Fig. 5. Dashed lines give the results with only three-phonon scattering, and solid lines give the results after including four-phonon scattering. Our calculated RT P for these materials are also given in Table II. Comparing AlSb, BAs, c-GaN, and w-GaN, we find that the isotope effect P is significantly weakened by four-phonon scattering, especially for AlSb. With only three-phonon scattering included, the largest P values occur for AlSb, with $P = 83.3\%$ at RT, and the calculated RT P values for BAs, c-GaN, and w-GaN are 46.0%, 51.2%, and 72.2–78.2%, respectively. Also, we note that for AlSb a peak in P occurs at around 200 K, which is attributed to the interplay between the anharmonic phonon-phonon scattering and the phonon-isotope scattering as mentioned before. With four-phonon scattering included, interestingly, we find that AlSb has the smallest P value among these materials, and its RT P decreases to 3.2%. In contrast, w-GaN shows the largest isotope effect among all the materials with $P = 56.8$–61.1% at RT; the next highest P is that of c-GaN, with $P = 37.2\%$ at RT; and the calculated RT P for BAs is ∼19.4%. These results are intriguing since four-phonon scattering can greatly weaken the isotope effect on κ for these materials with large a-o gaps, where the phonon-isotope scattering plays a significant or even dominant role over the anharmonic three-phonon scattering in determining κ.

E. Additional insights into four-phonon scattering

To understand the above results better, Fig. 6 gives the intrinsic three-phonon scattering rates τ_3^{-1}, the four-phonon scattering rates τ_4^{-1}, and the phonon-isotope scattering rates τ_{iso}^{-1} as a function of frequency for these four materials studied. We find that for AlSb and BAs τ_4^{-1} is very strong, comparable to or higher than τ_3^{-1} even at RT, and more so at 1000 K, especially for optical phonons, while τ_{iso}^{-1} is comparable to τ_3^{-1} at RT or lower temperatures [see Figs. 6(a) and 6(b)]. As T increases to 1000 K, the isotope scattering becomes relatively less important as compared to anharmonic phonon-phonon scattering, as shown in Figs. 6(e) and 6(f). The intrinsic phonon-phonon scattering rates scale with T as $AT + BT^2$, whereas the isotope scattering rates are T independent, causing the isotope effect to become less important with increasing T. Obviously, we can also see from Figs. 6(b) and 6(f) that in BAs the isotope scattering rates of optical modes are much larger than the three- and four-phonon scattering rates even at 1000 K, indicating that the isotope effect plays a dominant role in the optical phonon linewidths of BAs. As for c-GaN and w-GaN, as is seen in Figs. 6(c) and 6(d), the four-phonon scattering rates are much smaller than the three-phonon and isotope scattering rates at RT, but still cannot be neglected. When T goes up to 1000 K, we find that for both c-GaN and w-GaN the four-phonon scattering rates are comparable to the three-phonon scattering rates, as shown in Figs. 6(g) and 6(h). These results clearly demonstrate the importance of four-phonon scattering in determining κ for both naturally occurring materials and isotopically pure materials with a large band gap.

To gain a deeper understanding of four-phonon scattering, taking BAs and AlSb as examples, we further study the contribution to four-phonon scattering rates from all possible scattering channels. Clearly, we see from Figs. 7(a) and 7(c) that for both BAs and AlSb the dominant scattering channels for acoustic modes are the recombination processes $\mathbf{q} + \mathbf{q}_1 \longrightarrow \mathbf{q}_2 + \mathbf{q}_3 + \mathbf{k}$ and $\mathbf{q} + \mathbf{q}_1 \longrightarrow \mathbf{q}_2 + \mathbf{q}_3$ and the absorption process $\mathbf{q} + \mathbf{q}_1 + \mathbf{q}_2 \longrightarrow \mathbf{q}_3 + \mathbf{k}$, where $\mathbf{k}$ is a reciprocal lattice vector, which is zero for normal processes and nonzero for Umklapp processes. The dominant scattering channels for optical modes are the splitting process $\mathbf{q} \longrightarrow \mathbf{q}_1 + \mathbf{q}_2 + \mathbf{q}_3 + \mathbf{k}$ and the recombination processes $\mathbf{q} + \mathbf{q}_1 \longrightarrow \mathbf{q}_2 + \mathbf{q}_3 + \mathbf{k}$ and $\mathbf{q} + \mathbf{q}_1 \longrightarrow \mathbf{q}_2 + \mathbf{q}_3$. Amongst these scattering processes, the recombination process always makes a major contribution to τ_4^{-1}, whether acoustic or optical phonons. Due to the bunching of optical branches, these processes can easily satisfy the energy and momentum conservation rules, as illustrated in Fig. 1, unlike the absorption or splitting process, which strongly depends on the temperature T and the a-o gap. Also, we find that for both systems four-phonon scattering is dominated by resistive Umklapp processes as shown in Figs. 7(b) and 7(d), which also demonstrates the effectiveness of our iterative method described above.

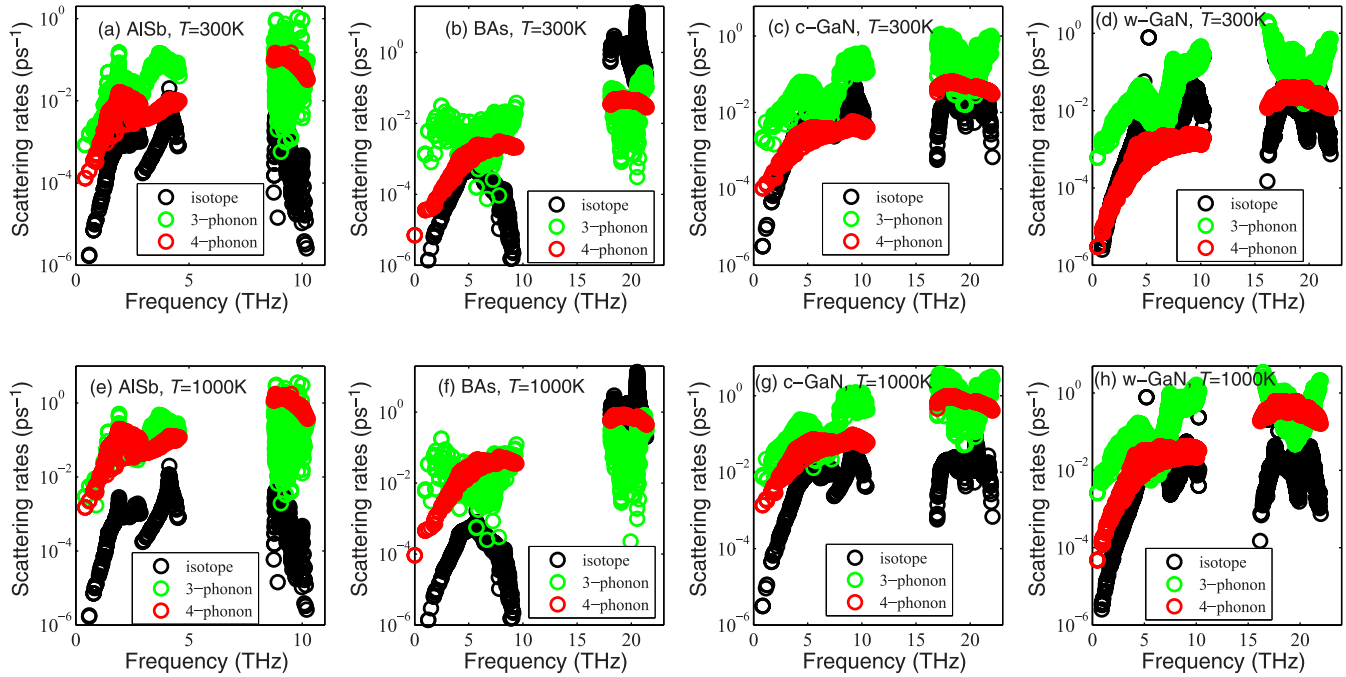

FIG. 6. Calculated intrinsic three-phonon scattering rates (green circles), four-phonon scattering rates (red circles), and the isotope scattering rates (black circles) as a function of frequency for AlSb (a, e), for BAs (b, f), for c-GaN (c, g), and for w-GaN (d, h) at 300 and 1000 K, respectively.

Moreover, to generalize the impact of four-phonon scattering on the κ of any solids, we normalize the a-o gap E_g by the highest LA phonon frequency ω_{LA} for ease of cross-comparing between different materials. Table IV lists the calculated Debye temperature θ_D, E_g, ω_{LA}, the normalized gap E_g/ω_{LA}, and the relative thermal conductivity $\kappa_{nat,3+4}/\kappa_{nat,3}$

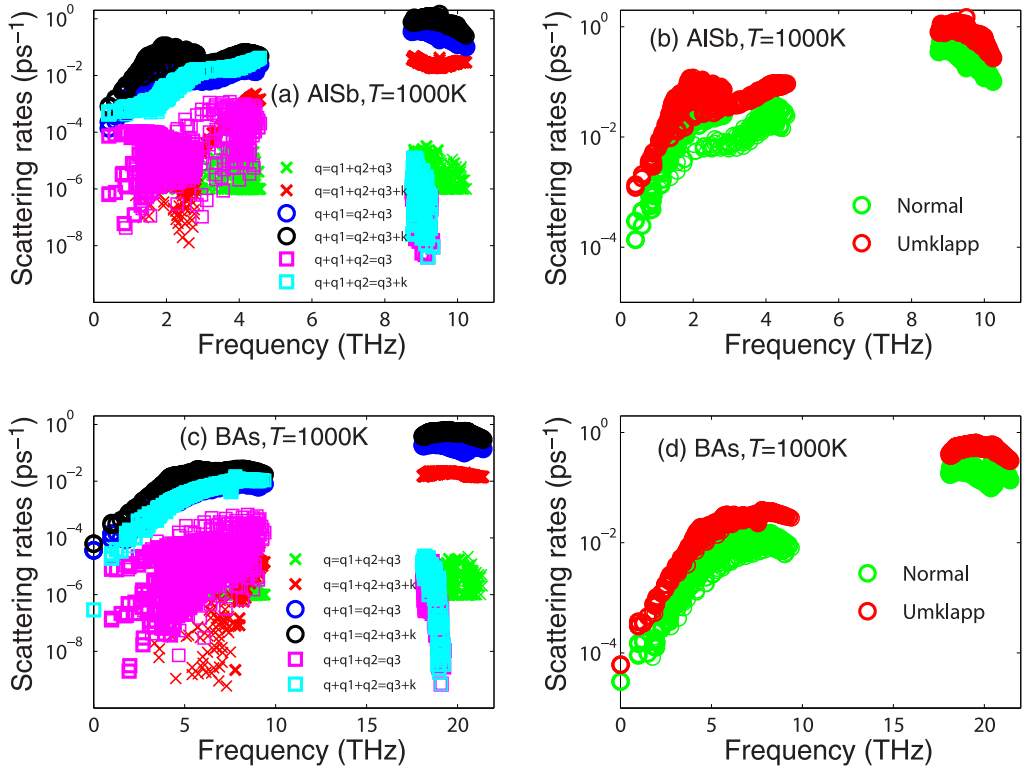

FIG. 7. The contribution to τ_4^{-1} from all allowed scattering channels as a function of frequency for AlSb (a) and BAs (c) at 1000 K. The contributions of Umklapp processes to τ_4^{-1} are compared to the contribution of normal processes for AlSb (b) and BAs (d) at 1000 K.

TABLE IV. Calculated Debye temperature θ_D, a-o gap E_g, highest LA phonon frequency, normalized a-o gap, and relative thermal conductivity $\kappa_{nat,3+4}/\kappa_{nat,3}$ at RT and $T = \theta_D$ in AlSb, BAs, c-GaN, and w-GaN.

Material	θ_D (K)	E_g (THz)	ω_{LA} (THz)	E_g/ω_{LA}	RT $\kappa_{nat,3+4}/\kappa_{nat,3}$ (%)	$\kappa_{nat,3+4}/\kappa_{nat,3}$ ($T = \theta_D$) (%)
AlSb	276	4.3	4.5	0.96	50.3	52.6
BAs	651	9.1	9.6	0.95	63.3	33.2
c-GaN	584	6.0	10.6	0.57	90.1	74.4
w-GaN (*a* axis)	584	6.1	9.4	0.65	97.7	88.7
w-GaN (*c* axis)	584	6.1	9.4	0.65	93.0	84.7

at RT and θ_D for materials studied in this work. Comparing AlSb, BAs, and c-GaN, which have the same crystal structure, we find that RT-$\kappa_{nat,3+4}/\kappa_{nat,3}$ increases monotonically with decreasing E_g/ω_{LA}, since the larger a-o gap, the weaker three-phonon scattering involving a-o coupling, leads to relatively more important four-phonon scattering, as demonstrated previously [18]. At $T = \theta_D$, however, $\kappa_{nat,3+4}/\kappa_{nat,3}$ does not change monotonically with the band gap. Typically, although E_g/ω_{LA} is larger in AlSb than in BAs, $\kappa_{nat,3+4}/\kappa_{nat,3}$ of BAs at $T = \theta_D$ is obviously smaller. The reason for this is that for BAs, besides the large a-o gap, the bunching of the acoustic band also restricts three-phonon interaction as mentioned above, which, however, cannot affect four-phonon processes. Also, by comparing between c-GaN and w-GaN, we find that, although they have almost same band gap, in c-GaN the thermal conductivity κ with τ_4^{-1} decreases by 25.6% at $T = \theta_D$, while the reduction of κ induced by τ_4^{-1} is less than 14% in the case of w-GaN. This can be explained from the difference in phonon dispersions of both materials. Comparing to c-GaN, in w-GaN there exist a few optical branches with frequency below the acoustic limit, as shown in Fig. 1. Although these optical modes do not significantly contribute directly to κ, they can provide important three-phonon scattering channels for the heat-carrying acoustic phonons, where four-phonon scattering is less important. Our analysis above indicates that the importance of four-phonon scattering depends not only on the a-o gap but also on the interplay among the a-o gap, the acoustic bunching, and the number of optical phonons with low frequency.

IV. CONCLUSIONS

To summarize, we employ a first-principles approach to revisit the κ and the isotope effect in AlSb, c-GaN, and w-GaN in comparison to BAs, by including four-phonon scattering. We demonstrate that in AlSb where three-phonon scattering involving optical phonons is extremely weak due to the unusual dispersion features (i.e., large a-o gap, the flatness of the optical bands), four-phonon scattering can actually play a dominant role in the optical phonon thermal resistance. Surprisingly, we find that four-phonon scattering completely diminishes optical phonon thermal conductivity and leads to ~50% reduction in the total κ of naturally occurring AlSb even at RT, which indicates a role of four-phonon scattering that is stronger than that in BAs. We believe this finding is not a special case but should exist in other semiconductor materials, which have phonon features similar to those of AlSb. Also, our calculation results show that four-phonon scattering can significantly weaken the relative role of the isotope effect on κ, especially for these materials with unusually weak anharmonic three-phonon scattering. Typically, for AlSb when four-phonon scattering is added, the isotope effect P at RT will be reduced significantly, from 83.2% to 3.2%. Furthermore, we demonstrate the general importance of four-phonon scattering in the intrinsic κ of materials, which is related to the interplay among the large a-o gap, the acoustic bunching, and low-frequency optical branches. Our work gives a critical revisit to exactly predicting the κ values of materials where optical phonons contribute considerably and also provides the rigorous understanding of the interplay between intrinsic phonon-phonon scattering and isotopic scattering.

ACKNOWLEDGMENTS

X.Y. acknowledges the support from the China Scholarship Council (Grant No. 201706280325). Simulations were performed at the Rosen Center of Advanced Computing at Purdue University and the Huashan No. 4 HPC cluster in State Key Laboratory for Mechanical Behavior of Materials at Xi'an Jiaotong University.

[1] S. Pearton, F. Ren, A. Zhang, G. Dang, X. Cao, K. Lee, H. Cho, B. Gila, J. Johnson, C. Monier *et al.*, Mater. Sci. Eng., B **82**, 227 (2001).
[2] K. Chung, C.-H. Lee, and G.-C. Yi, Science **330**, 655 (2010).
[3] A. L. Moore and L. Shi, Mater. Today **17**, 163 (2014).
[4] A. F. Al-Neama, N. Kapur, J. Summers, and H. M. Thompson, Appl. Therm. Eng. **140**, 622 (2018).
[5] A. Christensen, W. A. Doolittle, and S. Graham, IEEE Trans. Electron Devices **52**, 1683 (2005).
[6] D. A. Broido, M. Malorny, G. Birner, N. Mingo, and D. A. Stewart, Appl. Phys. Lett. **91**, 231922 (2007).
[7] J. Garg, N. Bonini, B. Kozinsky, and N. Marzari, Phys. Rev. Lett. **106**, 045901 (2011).
[8] A. Ward, D. A. Broido, D. A. Stewart, and G. Deinzer, Phys. Rev. B **80**, 125203 (2009).

[9] W. Li, N. Mingo, L. Lindsay, D. A. Broido, D. A. Stewart, and N. A. Katcho, Phys. Rev. B **85**, 195436 (2012).
[10] Z. Tian, J. Garg, K. Esfarjani, T. Shiga, J. Shiomi, and G. Chen, Phys. Rev. B **85**, 184303 (2012).
[11] X. Yang, J. Carrete, and Z. Wang, Appl. Phys. Lett. **108**, 113901 (2019).
[12] W. Li, L. Lindsay, D. A. Broido, D. A. Stewart, and N. Mingo, Phys. Rev. B **86**, 174307 (2012).
[13] L. Lindsay, D. A. Broido, and T. L. Reinecke, Phys. Rev. B **87**, 165201 (2013).
[14] L. Lindsay, D. A. Broido, and T. L. Reinecke, Phys. Rev. Lett. **109**, 095901 (2012).
[15] L. Lindsay, D. A. Broido, and T. L. Reinecke, Phys. Rev. Lett. **111**, 025901 (2013).
[16] E. F. Steigmeier and I. Kudman, Phys. Rev. **141**, 767 (1966).
[17] T. Feng and X. Ruan, Phys. Rev. B **93**, 045202 (2016).
[18] T. Feng, L. Lindsay, and X. Ruan, Phys. Rev. B **96**, 161201(R) (2017).
[19] T. Feng and X. Ruan, Phys. Rev. B **97**, 045202 (2018).
[20] J. S. Kang, M. Li, H. Wu, H. Nguyen, and Y. Hu, Science **361**, 575 (2018).
[21] S. Li, Q. Zheng, Y. Lv, X. Liu, X. Wang, P. Y. Huang, D. G. Cahill, and B. Lv, Science **361**, 579 (2018).
[22] F. Tian, B. Song, X. Chen, N. K. Ravichandran, Y. Lv, K. Chen, S. Sullivan, J. Kim, Y. Zhou, T.-H. Liu *et al.*, Science **361**, 582 (2018).
[23] Y. Xia, Appl. Phys. Lett. **113**, 073901 (2018).
[24] N. K. Ravichandran and D. Broido, Phys. Rev. B **98**, 085205 (2018).
[25] N. K. Ravichandran and D. Broido, Nat. Commun. **10**, 827 (2019).
[26] D. A. Broido, L. Lindsay, and A. Ward, Phys. Rev. B **86**, 115203 (2012).
[27] J. M. Ziman, *Electrons and Phonons*, Oxford Classic Texts in Physical Sciences (Oxford University, Oxford, 1960).
[28] W. Li, J. Carrete, N. A. Katcho, and N. Mingo, Comput. Phys. Commun. **185**, 1747 (2014).
[29] K. Esfarjani, G. Chen, and H. T. Stokes, Phys. Rev. B **84**, 085204 (2011).
[30] G. Kresse and J. Hafner, Phys. Rev. B **47**, 558 (1993).
[31] G. Kresse and J. Furthmüller, Comput. Mater. Sci. **6**, 15 (1996).
[32] G. Kresse and J. Furthmuller, Phys. Rev. B **54**, 11169 (1996).
[33] A. Togo, F. Oba, and I. Tanaka, Phys. Rev. B **78**, 134106 (2008).
[34] Aluminum antimonide (AlSb), lattice parameter, thermal expansion, in *Group IV Elements, IV-IV and III-V Compounds. Part b - Electronic, Transport, Optical and Other Properties*, Landolt-Börnstein - Group III Condensed Matter, Vol. 41A1β, edited by O. Madelung, U. Rössler, and M. Schultz (Springer-Verlag, Berlin, Heidelberg, 2002).
[35] O. Lagerstedt and B. Monemar, Phys. Rev. B **19**, 3064 (1979).
[36] Aluminum antimonide (AlSb) phonon dispersion, phonon wavenumbers, in *Group IV Elements, IV-IV and III-V Compounds. Part a - Lattice Properties*, Landolt-Börnstein - Group III Condensed Matter, Vol. 41A1α, edited by O. Madelung, U. Rössler, and M. Schulz (Springer-Verlag, Berlin, Heidelberg, 2001).
[37] A. Jeowski, P. Stachowiak, T. Plackowski, T. Suski, S. Krukowski, M. Bokowski, I. Grzegory, B. Danilchenko, and T. Paszkiewicz, Phys. Status Solidi B **240**, 447 (2003).
[38] Q. Zheng, C. Li, A. Rai, J. H. Leach, D. A. Broido, and D. G. Cahill, Phys. Rev. Mater. **3**, 014601 (2019).